Nanoreactors

DOI: 10.1002/anie.200801606

An Integrated Self-Assembled Nanofluidic System for Controlled Biological Chemistries**

*Pierre-Yves Bolinger, Dimitrios Stamou, and Horst Vogel**

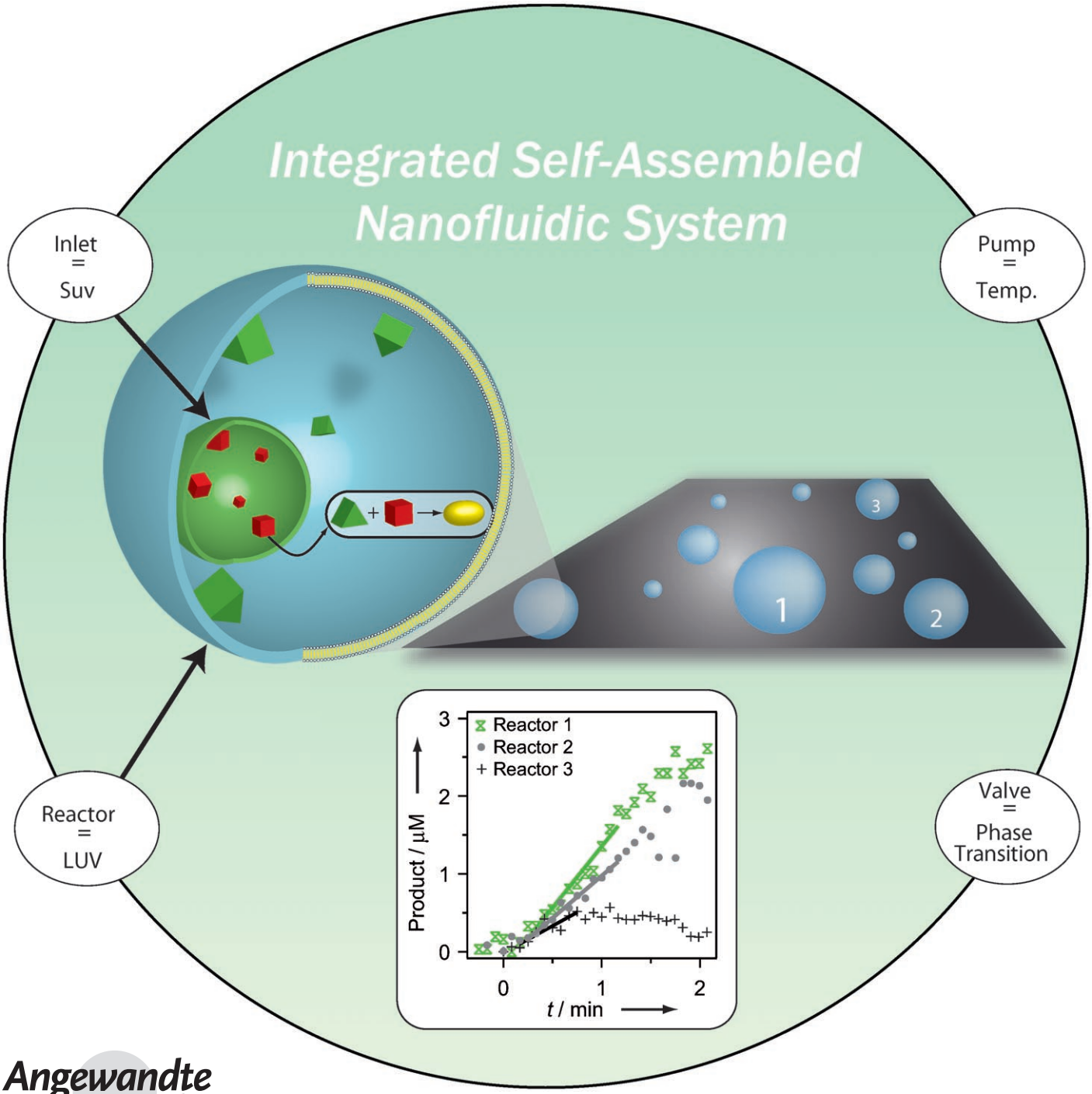

The strong biotechnological drive for miniaturized reaction systems to reduce sample consumption and increase throughput has, to date, been mainly addressed by microfabrication.[1–4] Herein, we use self-assembly (SA)[5,6] to create a nanofluidic system for mixing attoliter volumes (released from nanometer-sized lipid vesicles) in a closed femtoliter reactor vessel (a larger unilamellar lipid vesicle), thereby controlling the number of mixed reactants with single-molecule precision. The reactions are monitored in situ by fluorescence correlation spectroscopy (FCS). The mixing of reactants, which initiates an enzyme-catalyzed transformation of nonfluorescent substrate to a fluorescent product, is triggered by changes in temperature that drive the small vesicles through phase transitions.[7,8] The closed, autonomous nanoreactor allows repetitive addition of reactants and successive distinct reactions; the system remains tightly sealed for weeks. This approach opens novel vistas for ultra-miniaturized screening of chemical and protein libraries, synthetic chemistry and biology, and for constructing artificial cells.

Chemical reactions inside biological cells occur on 3D length scales ranging from several micrometers to nanometers, as dictated by the dimensions of cells and their intracelluar compartments. Biological systems employ molecular SA as a ubiquitous method to create highly complex and functionally efficient nanoscale architectures for establishing the cellular biochemical network.[5a] The biological miniaturization and complexity of biochemical processes is unmatched in laboratory synthetic chemistry. For example, the most important laboratory manipulation to initiate a chemical reaction is the mixing of defined volumes and concentrations of reactants inside a reactor of defined size. What is trivial at macroscopic scale becomes an unsolved challenge if mixing should be downscaled to sub-femtoliter volumes. Present microtechnologies are capable of handling volumes as small as 50 fL.[1–4] Alternatively, self-assembled vesicles made of polypeptides, polymers, or lipids have evolved to enclose small volumes.[6,9–16]

[*] Dr. P.-Y. Bolinger, Prof. H. Vogel
Institut des Sciences et Ingénierie Chimiques
Ecole Polytechnique Fédérale de Lausanne
1015 Lausanne (Switzerland)
Fax: (+41) 21-6936190
E-mail: horst.vogel@epfl.ch
Dr. P.-Y. Bolinger, Prof. D. Stamou
Bio-Nanotechnology Laboratory
Department of Neuroscience and Pharmacology &
Nano-Science Centre
University of Copenhagen
Universitetsparken 5, 2100 Copenhagen (Denmark)

[**] We thank N. Hatzakis, C. Danelon, and R. Trend for critically reading the manuscript and A. O. Dohn for the cover artwork. This work was performed at the EPFL (PhD thesis of P.Y.B.), funded by the TopNano21 programme and EPFL grants to H.V. We also acknowledge support from the Danish Research Councils to D.S. and postdoctoral fellowships from the Danish Research Councils and the Swiss National Foundation to P.Y.B.

Supporting information for this article is available on the WWW under http://dx.doi.org/10.1002/anie.200801606.

Especially lipid vesicles offer interesting advantages, including 1) fast and cheap production, 2) biocompatibility, and 3) ultra-miniaturization to zeptoliter volumes (10^{-21} L).[6,7,12–16] Their potential relevance for carrying out confined reactions in individual containers[7,13] has not been fully exploited, mainly owing to lack of control, reproducibility in their fabrication, and functional complexity. Herein we present one of the most complex, functional self-assembled nanofluidic systems, optimized for initiating and monitoring biochemical reactions.

Figure 1 illustrates conceptually our nanofluidic system. The choice of lipids with a specific ordered-fluid phase-transition temperature (T_t) enabled us to define accurately the temperature under which the small unilamellar vesicles (SUVs), trapped in the interior of a large unilamellar vesicle (LUV), release their cargo. This cargo is subsequently confined and mixed in the interior of the LUV, which serves as a chemical nanoreactor. Furthermore, by incorporating different sorts of SUVs with different T_t, different compounds can be released in succession at each particular T_t, thus allowing the controlled, consecutive initiation of distinct chemical reactions within the same nanoreactor. To monitor the function of the individual reactor systems in a parallel manner, biotinylated nanoreactors are immobilized on a solid support functionalized with neutravidin. The use of biotin-PEG-lipids with long poly(ethylene glycol) (PEG) spacers prevents nanoreactor destabilization or destruction. To increase the lifetime of the reactors, we also employed negatively charged lipids to create an electrostatic repulsive barrier that keeps the SUVs "suspended" in the nanoreactor by suppressing interactions with other SUVs or with the walls of the reactor, which could cause uncontrolled leakage. We found that SUVs composed of DPPC/DPPG = 9:1 molar ratio (DPPC = dipalmitoylphosphatidylcholine, DPPG = dipalmitoylphosphatidylglycerol) were efficiently enclosed into the lumen of the nanoreactors.

To demonstrate a potential application of our system, we focused on enzyme catalysis as a class of key biochemical reactions for the biological function of a cell. Alkaline phosphatase (AP) was chosen as a prototypical enzyme of biological relevance that regulates a variety of cellular signal transduction pathways.[17] Figure 2a,b shows confocal microscopy images of nanoreactors immobilized on a glass plate before and after the release of nonfluorescent substrate FDP that reacted with AP to be converted to a fluorescent product (fluorescein). Figure 2c illustrates product formation starting a few degrees below the SUVs' lipid phase-transition temperature $T_t = 41\,^{\circ}C$ (determined by differential scanning calorimetry), as observed previously in a different context.[7] The time course (i.e. temperature dependence) of the product's fluorescence intensity in a single nanoreactor and averaged over 20 nanoreactors is similar, demonstrating that the release process occurs at a precise temperature and is highly reproducible for all reactors.

FCS is used to determine the concentration of reactants and products inside the lumen of individual reactors. A laser beam focused into an individual nanoreactor probes the number and the mobilities of single fluorescent molecules and SUVs diffusing across the subfemtoliter-sized confocal

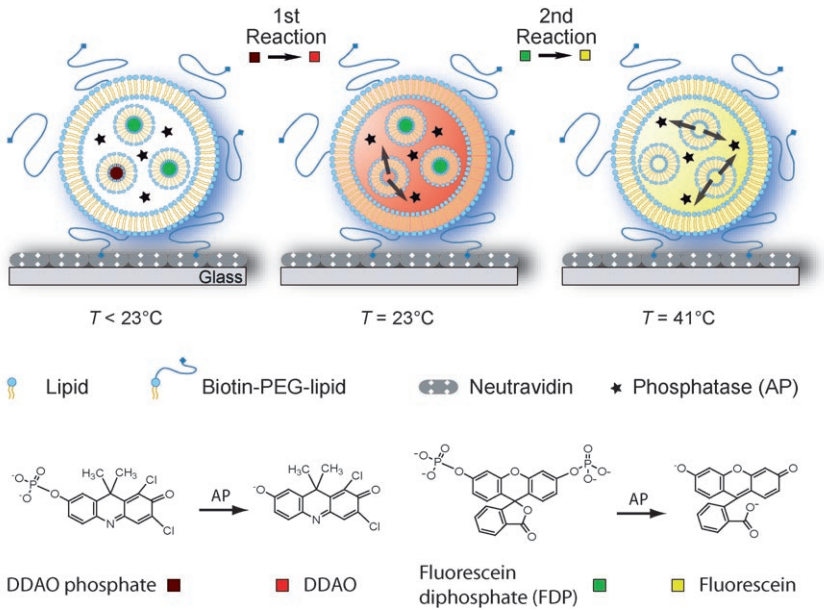

Figure 1. Consecutive enzymatic reactions in a single nanoreactor. The external nanoreactor surface comprises biotin for immobilization on a neutravidin-coated glass slide. Alkaline phosphatase (AP, star) is incorporated in the nanoreactor together with two kinds of SUVs, each loaded with a different nonfluorescent substrate for the enzyme. The first kind of SUV ($T_t \approx 23\,°C$) is loaded with dichlorodimethylacridinone (DDAO) phosphate (dark red) and the second kind of SUV ($T_t \approx 41\,°C$) is loaded with fluorescein diphosphate (FDP, dark green). An increase of temperature triggers the release of the substrates in two distinct, consecutive steps at the two corresponding phase-transition temperatures, first DDAO phosphate at 23 °C and then FDP at 41 °C. After release from the SUVs, the substrates remain confined in the nanoreactor, where they are converted by the enzyme to their particular fluorescent products, DDAO (light red) and FDP (light green).

volume, thus enabling us to distinguish freely diffusing dye molecules from those encapsulated in SUVs using their autocorrelation functions, as shown elsewhere (Figure 2d,e).[18,19] Figure 2d shows the autocorrelation function $G(t)$ of Alexa 488 dye before (black) and after (green) release from SUVs inside individual nanoreactors. After release, no encapsulated, slow-diffusing dye could be detected, thus indicating a release efficiency of approximately 100%. To demonstrate the potential of our nanoreactors for quantitative chemistry, two different preparations of nanoreactors containing SUVs loaded with either low (3.2 μM) or high (32 μM) initial dye concentration (corresponding to an average of 1 or 13 dye molecules per SUV) were analyzed before and after heating above T_t. Consistent results were obtained: 1) The number of dye molecules released from SUVs loaded with 3.2 μM was identical with the number of SUVs before heating. As each SUV initially contained on average one dye molecule, the releasing efficiency is close to 100%. Unheated SUVs did not show significant passive leakage over two weeks after production. 2) As expected, the average number of dye moleucles released from highly loaded SUVs (average of 13 dye molecules per SUV) is ten times higher than the number of SUVs before heating and ten times higher than the number of dye molecules released from SUVs loaded with one dye molecule per SUV. 3) Increasing the concentration of entrapped dye did not affect the number of incorporated SUVs in a nanoreactor. The encapsulation of dye in SUVs is fairly uniform. The standard deviation in the concentration of released dye is therefore mainly due to the variation of loading nanoreactors with SUVs. The high release efficiency is a consequence of the large dilution upon release (ca. 2000 fold) and the complete suppression of nonspecific interactions between the SUVs' hydrophobic membrane and the hydrophilic dye. Results shown in Figure 2d,e demonstrate the reliability of production of the nanoreactor system by SA, the substrate release, and consequently, the final concentration of the substrate in the nanoreactor vessel.

To demonstrate the enzymatic transformation principle, a control experiment is shown Figure 2f. Two sorts of nanoreactors were produced and analyzed. One was loaded with substrate-containing SUVs together with enzyme; the other was loaded with substrate-containing SUVs but without enzyme. A fluorescent lipid (ex 550, em 590 nm) inserted in the membrane of the second sort of nanoreactor distinguishes the two vesicle populations. The different nanoreactors were finally mixed, immobilized on the microscope slide, and heated to release the substrate. The fact that we observe temperature-induced fluorescence changes only in the nanoreactors which contain enzymes confirms that the fluorescence changes stem from the enzymatic reaction. The stable signal of the membrane dye before and after release indicates that temperature scans did not move the sample out of focus.

In the following, we quantitatively evaluate the enzyme kinetics in the individual nanoreactors. Figure 3a shows the time course of product formation (fluorescein from FDP) inside three different nanoreactors at approximately 0.4 μM enzyme concentration. The reaction between enzyme (E) and substrate (S) in the LUV nanoreators is described by Equation (1), where k_1 and k_{-1} are the rate constants for

$$S + E \underset{k_{-1}}{\overset{k_1}{\rightleftharpoons}} C \xrightarrow{k_2} P \qquad (1)$$

formation and dissociation of the enzyme–substrate complex (C), and k_2 is the rate constant of the formation of product (P). Under our experimental conditions of relatively low total concentrations of substrate over enzyme $[S_0]/[E_0] \approx 1$–10, the rate V of product formation can be described by Equation (2)

$$V = k_2/2(([S_0] + [E_0] + K_M) - (([S_0] + [E_0] + K_M)^2 - 4([S_0]\,[E_0]))^{1/2}) \qquad (2)$$

with the Michaelis constant K_M.[20] From the dependence of the rate of product formation on the total concentration of substrate transformed (Figure 3b) and a fit with Equation (2), we obtained values of $K_M = 0.6 \pm 0.2$ μM and $k_2 = 4.2 \pm$

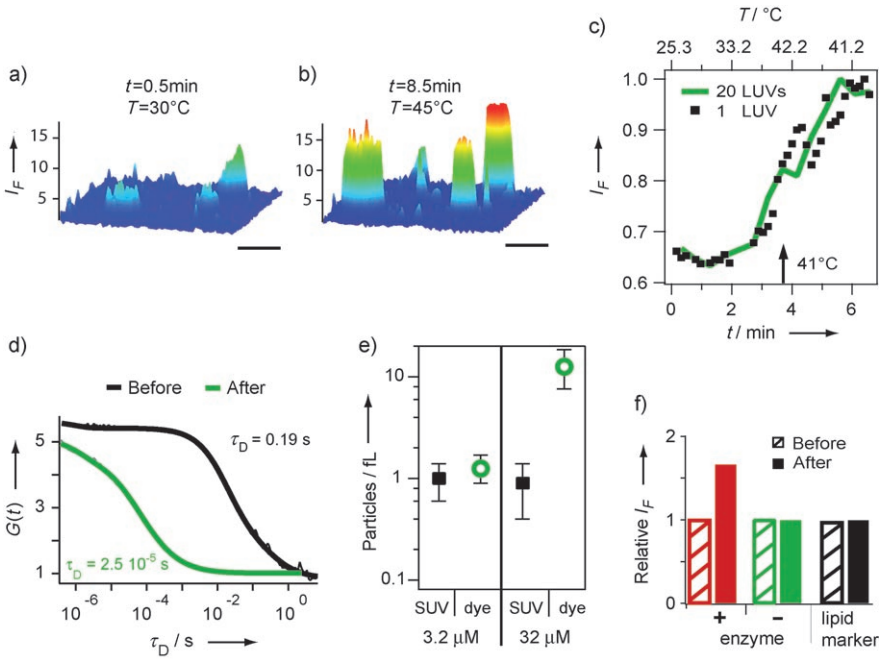

Figure 2. Quantitatification of nanoreactor production and operational performance. Lipid composition of SUVs was DPPC/DPPG = 9:1; that of nanoreactors was DOPG (dioleoylphosphatidylglycerol). a–c) Triggered release of FDP inside nanoreactors and its conversion to a fluorescent product by AP. Fluorescence images of nanoreactors (excitation 480, emission 520 nm; scale bars 10 µm): Fluorescence intensity as color code on vertical axis is plotted for each pixel in the focal plane a) before (30 °C) and b) after (45 °C) release of FDP inside the nanoreactors. Initial concentration before encapsulation is FDP 0.5 mM and AP 175 nM. c) Time course of the fluorescence intensity inside single nanoreactors corresponding to the enzymatic conversion of nonfluorescent substrate FDP into fluorescent product fluorescein. One reactor (squares) is compared to the average of 20 reactors (green line). Data were extracted from a single $100\times100\ \mu m^2$ field of view. d), e) FCS measurements. d) Autocorrelation function $G(t)$ of Alexa 488 before (black) and after (green) release from SUVs inside single nanoreactors. e) In situ quantification of the number of released dye molecules as a function of the concentration of encapsulated SUVs and encapsulated dye molecules. Each point represents an average of several (ca. 10) individual nanoreactors. For an initial dye concentration of 3.17 mM inside the SUVs (average of 1.3 dye molecules per SUV), the total number of released dye moleucles (green circles) equals the number of SUVs (black squares). A tenfold increase of the initial dye concentration inside the SUVs to 31.7 mM while keeping the number of SUVs constant also increased the number of released dye molecules tenfold. f) Control experiment using two sorts of nanoreactors, one loaded with substrate-containing SUVs together with enzyme (+), the other loaded with substrate-containing SUVs but without enzyme (−).

$0.4\ min^{-1}$. We measured very similar values ($K_M = 0.4 \pm 0.2\ \mu M$ and $k_2 = 4.0 \pm 0.3\ min^{-1}$) for the enzymatic reaction in bulk solution under the same conditions as used in the nanoreactors (pH value, temperature, enzyme and substrate concentrations), thus demonstrating the high performance and reliability of the single-nanoreactor experiments despite the extremely small quantities of reagents used (for 1–10 µm LUVs: 10^{-17}–10^{-14} g enzyme, 10^{-18}–10^{-15} g substrate).

In addition to single-step enzyme reactions, the nanofluidic system can serve as a closed, autonomous nanoreactor performing consecutive multistep enzyme reactions. As a proof of principle, we prepared a system in which each nanoreactor enclosed two different sorts of SUVs distinguished by different T_t and different enclosed nonfluorescent substrates for AP, DDAO phosphate, and FDP. Figure 3c depicts the confocal images and the corresponding time courses of two enzymatic reactions within one single nanoreactor. In Figure 3d, the red time course shows the increase of fluorescence intensity at approximately 23 °C arising form the release of DDAO phosphate from DMPC/DMPG = 4:1 SUVs (DMPC = dimyristoylphosphatidylcholine) and its enzymatic transformation to highly fluorescent DDAO. The green time course corresponds to the enzymatic reaction resulting from the release of FDP from DPPC/DPPG = 9:1 SUVs and its transformation to fluorescein. The results shown in Figure 3c,d reveal that the two enzymatic reactions occurred consecutively and in a highly controlled manner within the same nanoreactor. The temperature width of approximately 6 °C over which the substrate release takes place consequently would allow the sequential triggering of as many as four reactions within a temperature range of approximately 25 °C.

Because mixing of reactants is remotely triggered by changes in temperature, the LUVs function as fully autonomous nanoreactors without the need for external interfacing of the reactor (e.g. outlets and inlets or extra fusion steps between different containers), allowing for extreme miniaturization. We prepared nanoreactors with controlled diameters between 1 and 10 µm that enclosed cargo SUVs with an average diameter of about 100 nm (as determined by quasi-elastic light scattering and electron microscopy). Consequently, we varied the volume of our nanoreactors from 1 to 1000 fL, while the individual SUVs had attoliter volumess. Though the fabrication process is based on hierarchical SA, we had quantitative control over both the assembly of the reactors (concentration variability of reactants ±30%) and their operational performance (release efficiency of reactants ca. 100%). The release of the cargo molecules from the SUVs inside a nanoreactor could be finely controlled in several ways leading to a stepwise addition of reactants from a few to hundreds of molecules per nanoreactor: 1) by the concentration of cargo molecules inside the SUVs (typically controlled between 1 and 20 molecules per SUV), 2) by the number of SUVs enclosed inside a nanoreactor (typically controlled between 1 and 100 fL^{-1}), 3) by the rate of release of the cargo molecules from the SUVs into the lumen of the nanoreactor. The rate can be controlled by the rate of temperature change and might lead, in the case of fast temperature jumps,[11e] to multiple cargo releases from the same population of SUVs inside a particular nanoreactor

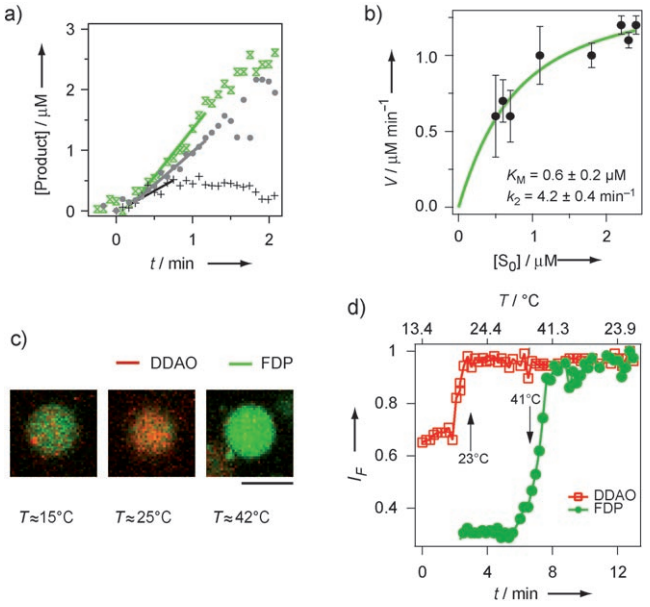

Figure 3. Kinetics and multiplexing of enzymatic reactions in different individual LUV nanoreactors within one field of view. a) Time course of product formation for three different nanoreactors containing total substrate concentrations [S_0] = 0.5 μM (+), 2 μM (●), 3 μM (×). The initial reaction rate V is determined for a particular substrate concentration [S_0] inside a nanoreactor by fitting the time course of product formation linearly after the inflection when substrate is released from SUVs. b) Dependence of V on [S_0]; each data point corresponds to one individual nanoreactor (total 8). Fitting the data by Equation (2) (green line) yields k_2 and K_M. c) Two consecutive reactions in a single LUV nanoreactor. LUV was loaded with two kinds of SUVs, one made of DMPC/DMPG = 4:1 (DMPG = dimyristoylphosphatidylglycerol) (T_t = 23 °C) and encapsulating DDAO phosphate, the other made of DPPC/DPPG = 9:1 (T_t = 41 °C) and containing FDP. Scale bar 10 μm. d) Consecutive release of the two different substrates at the different lipid phase-transition temperatures during one temperature scan.

corresponding to repetitive titrations steps. Lipid phase transitions can be also induced by changes of the ionic environment (e.g. pH value, Ca^{2+} concentration),[21] pressure, or electrical fields,[22] thus opening the possibility to release reactants inside the nanoreactor isothermally and transiently.

Our technology resembles in many respects the performance known from classical macroscopic synthetic chemistry. The ability to add molecules repetitively in a finely controlled manner to the nanoreactor vessel shows that titrations can be performed on this small scale. Distinct reactions can be initiated consecutively. The reactors are tightly sealed over long time periods. They can be locally trapped, as demonstrated herein, on a glass surface by specific and strong interaction between avidin–biotin or other procedures known from multiarray technologies.[23] It has been shown elsewhere that vesicles could also be immobilized in a reversible manner, either chemically on surfaces[24] or free-floating by using optical tweezers.[25] This approach enables, in addition, the transport of nanoreactors in microfluidic devices over macroscopic distances without loss of enclosed molecular components, for example to sort and collect them in nanofactories.[5,25b] We have also shown that nanoreactors can be immobilized as ensembles to perform and characterize chemical syntheses simultaneously in a highly parallel manner. In this context, multiple optical traps offer additional advantages for miniaturized immobilization and monitoring.[23,25b] Apart from dramatically downscaling the consumption of reagents, the lipid-based reactors are compatible with many cellular biochemistries. This feature offers the possibility to combine the artificial lipid vesicles with cell-derived native vesicles, which carry both cellular membrane and cytoplasmic components.[26] One or the other sort of vesicle could be used as nanoreactor or SUV, thus opening new possibilities for synthetic biology. The feature that our nanoreactors are totally autonomous, enclosing smaller entities which can selectively release their cargo upon a trigger to initiate complex reactions, resembles cells with intracellular compartments (organelles) and thus adds an essential component for constructing artificial cells by self-organization.[27]

Experimental Section

See the Supporting Information for details.

Received: April 6, 2008

Keywords: biomimetic systems · nanochemistry · nanoreactors · nanotechnology · vesicles

[1] a) E. Delamarche, A. Bernard, H. Schmid, B. Michel, H. Biebuyck, *Science* **1997**, *276*, 779; b) E. Delamarche, D. Juncker, H. Schmid, *Adv. Mater.* **2005**, *17*, 2911.
[2] a) P. S. Dittrich, A. Manz, *Nat. Rev. Drug Discovery* **2006**, *5*, 210; b) D. Janasek, J. Franzke, A. Manz, *Nature* **2006**, *442*, 374; c) G. M. Whitesides, *Nature* **2006**, *442*, 368.
[3] a) D. M. Rissin, D. R. Walt, *J. Am. Chem. Soc.* **2006**, *128*, 6286; b) H. H. Gorris, D. M. Rissin, D. R. Walt, *Proc. Natl. Acad. Sci. USA* **2007**, *104*, 17680.
[4] S. Sauer, B. M. H. Lange, J. Gobom, L. Nyarsik, H. Seitz, H. Lehrach, *Nat. Rev. Genet.* **2005**, *6*, 465.
[5] a) G. M. Whitesides, B. Grzybowski, *Science* **2002**, *295*, 2418; b) S. Zhang, *Nat. Biotechnol.* **2003**, *21*, 1171.
[6] a) S. M. Christensen, D. Stamou, *Soft Matter* **2007**, *3*, 828; b) Y. H. M. Chan, S. G. Boxer, *Curr. Opin. Chem. Biol.* **2007**, *11*, 581.
[7] P. Y. Bolinger, D. Stamou, H. Vogel, *J. Am. Chem. Soc.* **2004**, *126*, 8594.
[8] O. G. Mouritsen, *Life—As a Matter of Fat*, Springer, Berlin, **2005**.
[9] S. Santoso, W. Hwang, H. Hartman, S. G. Zhang, *Nano Lett.* **2002**, *2*, 687.
[10] H. C. Chiu, Y. W. Lin, Y. F. Huang, C. K. Chuang, C. S. Chern, *Angew. Chem.* **2008**, *120*, 1813; *Angew. Chem. Int. Ed.* **2008**, *47*, 1789.
[11] a) C. Yoshina-Ishii, S. G. Boxer, *J. Am. Chem. Soc.* **2003**, *125*, 3696; b) S. Svedhem, I. Pfeiffer, C. Larsson, C. Wingren, C. Borrebaeck, F. Hook, *ChemBioChem* **2003**, *4*, 339; c) M. R. Dusseiller, B. Niederberger, B. Stadler, D. Falconnet, M. Textor, J Voros, *Lab Chip* **2005**, *5*, 1387; d) D. Peer, J. M. Karp, S. Hong, O. C. Farokhzad, R. Margalit, R. Langer, *Nat. Nanotechnol.* **2007**, *2*, 751; e) G. B. Sukhorukov, A. L. Rogach, M. Garstka, S. Springer, W. J. Parak, A. Muoz-Javier, O. Kreft, A. G. Skirtach, A. S. Susha, Y. Ramaye, R. Palankar, M. Winterhalter, *Small* **2007**, *3*, 944.

[12] D. M. Vriezema, M. C. Aragones, J. Elemans, J. Cornelissen, A. E. Rowan, R. J. M. Nolte, *Chem. Rev.* **2005**, *105*, 1445.
[13] D. Stamou, C. Duschl, E. Delamarche, H. Vogel, *Angew. Chem.* **2003**, *115*, 5738; *Angew. Chem. Int. Ed.* **2003**, *42*, 5580.
[14] D. S. Tawfik, A. D. Griffiths, *Nat. Biotechnol.* **1998**, *16*, 652.
[15] a) I. Cisse, B. Okumus, C. Joo, T. J. Ha, *Proc. Natl. Acad. Sci. USA* **2007**, *104*, 12646; b) P. S. Dittrich, M. Jahnz, P. Schwille, *ChemBioChem* **2005**, *6*, 811; c) A. Karlsson, K. Sott, M. Markstrom, M. Davidson, Z. Konkoli, O. Orwar, *J. Phys. Chem. B* **2005**, *109*, 1609; d) L. Lizana, B. Bauer, O. Orwar, *Proc. Natl. Acad. Sci. USA* **2008**, *105*, 4099.
[16] P. Walde, S. Ichikawa, *Biomol. Eng.* **2001**, *18*, 143.
[17] V. Janssens, J. Goris, *Biochem. J.* **2001**, *353*, 417.
[18] P. Rigler, W. Meier, *J. Am. Chem. Soc.* **2006**, *128*, 367.
[19] E. Boukobza, A. Sonnenfeld, G. Haran, *J. Phys. Chem. B* **2001**, *105*, 12165.
[20] M. Blocher, P. Walde, I. J. Dunn, *Biotechnol. Eng.* **1999**, *62*, 36.
[21] H. Trauble, H. Eibl, *Proc. Natl. Acad. Sci. USA* **1974**, *71*, 214.
[22] B. Gruenewald, A. Blume, F. Watanabe, *Biochim. Biophys. Acta Biomembr.* **1980**, *597*, 41.
[23] C. N. LaFratta, D. R. Walt, *Chem. Rev.* **2008**, *108*, 614.
[24] T. Stora, Z. Dienes, H. Vogel, C. Duschl, *Langmuir* **2000**, *16*, 5471.
[25] a) D. T. Chiu, C. F. Wilson, A. Karlsson, A. Danielsson, A. Lundqvist, A. Stromberg, F. Ryttsen, M. Davidson, S. Nordholm, O. Orwar, R. N. Zare, *Chem. Phys.* **1999**, *247*, 133; b) F. Merenda, J. Rohner, P. Pascoal, J. M. Fournier, H. Vogel, R. P. Salathé, *Proc. SPIE-Int. Soc. Opt. Eng.* **2008**, *6483*.
[26] H. Pick, E. L. Schmid, A. P. Tairi, E. Ilegems, R. Hovius, H. Vogel, *J. Am. Chem. Soc.* **2005**, *127*, 2908.
[27] a) V. Noireaux, A. Libchaber, *Proc. Natl. Acad. Sci. USA* **2004**, *101*, 17669; b) V. Noireaux, R. Bar-Ziv, J. Godefroy, H. Salman, A. Libchaber, *Phys. Biol.* **2005**, *2*, P1.

